Quasioptical phase cycling in a free electron laser-powered pulsed electron paramagnetic resonance spectrometer: Supporting Information

Christopher B. Wilson,[1,2] Samuel Aronson,[1] Jessica A. Clayton,[1,2] Steffen J. Glaser,[3] Songi Han,[2,4] and Mark S. Sherwin[1,2]

[1]*Department of Physics, University of California, Santa Barbara, Santa Barbara, California, USA*

[2]*Institute for Terahertz Science and Technology, University of California, Santa Barbara, Santa Barbara, California, USA.*

[3]*Department of Chemistry, Technical University of Munich, Garching, Germany*

[4]*Department of Chemistry and Biochemistry, University of California, Santa Barbara, Santa Barbara, California, USA*

(Dated: March 22, 2018)

PRODUCTION AND CHARACTERIZATION OF DIELECTRIC PHASE SHIFTER PLATES

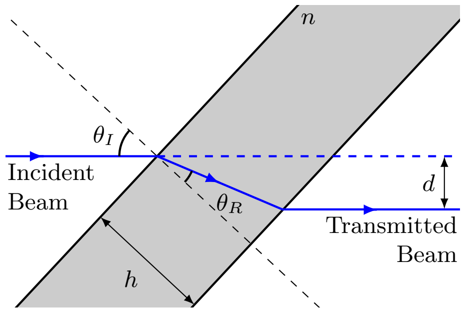

FIG. S1: Schematic of a THz beam, shown in blue, incident with angle Θ_I on a slab of thickness h with refractive index n. The material on either side of the slab is taken to be air, with a refractive index of 1. After propagating through the slab, the beam is deflected a distance d.

Phase shifter plates were constructed out of high density polyethylene (HDPE), which is transparent to 240 GHz radiation[1, 2] and can be machined to precise tolerances. Figure S1 shows the path taken by a 240 GHz beam as it passes through a phase shifter plate of thickness h and refractive index n, with an angle of incidence Θ_I. The optical path length difference ΔOPL introduced by the phase shifter plate is given by

$$\Delta OPL = \frac{nh}{\cos\Theta_R} - \frac{h}{\cos\Theta_R}\cos\left(\Theta_I - \Theta_R\right) \tag{1}$$

where Θ_I and Θ_R are related by Snell's law, giving

$$\Delta OPL = h\left(n\sqrt{1 - \frac{\sin^2\Theta_I}{n^2}} - \cos\Theta_I\right) \tag{2}$$

At the Brewster angle $\tan\Theta_I = n$, and Equation 2 reduces to

$$\Delta OPL = h\frac{n^2 - 1}{\sqrt{n^2 + 1}} \tag{3}$$

The phase shift ϕ picked up by the 240 GHz beam as it traverses the phase shifter plate is given by

$$\phi = 2\pi\frac{\Delta OPL}{\lambda_0} \tag{4}$$

where $\lambda_0 = 1.249$ mm is the wavelength of 240 GHz radiation in free space.

In addition to picking up a phase shift ϕ, the transmitted 240 GHz beam is offset by a distance d given by

$$d = h \sin \Theta_I \left(1 - \frac{\sin \Theta_I / n}{\sqrt{1 + \sin^2 \Theta_I / n^2}} \right) \tag{5}$$

At the Brewster angle, Equation 5 becomes

$$d = \frac{h}{n} \frac{n^2 - 1}{\sqrt{n^2 + 1}} \tag{6}$$

Phase shifter plates were used in pairs to reduce the beam offset d.

COHERENT SIGNAL AVERAGING AND MEASUREMENTS OF PULSE PHASES

The phase of each long FEL pulse is random, making coherent signal averaging challenging. Coherent signal averaging was accomplished using the technique developed by Edwards *et al.*[3] First, the time-domain signal of each experiment is recorded and stored separately. Included in the recorded signals are the digitized pulses themselves, from which some residual light "leaks" through our spectrometer's isolation. Residual light from the second short pulse is used to measure the overall phase of the long FEL pulse, and a phase shift is applied to each separately recorded signal to remove this overall phase. After this first phase correction, the phase of the first short sliced pulse was measured using the same technique, utilizing residual light from the first pulse. Phase determination and correction are described in detail in Edwards *et al.*[3] Routines were implemented in LabView.

OPTIMIZING RECEIVER PHASES TO MINIMIZE UNWANTED COHERENCES

The general problem can be summarized as follows: given a set of four phases applied to the first pulse in a two-pulse experiment, what is the optimal choice of receiver phases to apply in post-processing, to both maximally attenuate unwanted coherences and maximally preserve desired coherences? This is different from the scenario typically encountered in magnetic resonance experiments, where the optimal choices of pulse and receiver phases are made together. Phase shifts applied using POPS to the first pulse as implemented here are imposed by hardware. The specific pulse phases are limited by machining tolerances in the phase shifter plates, and by how reproducibly the phase shifter plates can be placed in the experimental setup.

In a two-pulse FEL-EPR experiment with four-step POPS, we consider three coherence transfer pathways, which we label by the coherence order change Δp during the first pulse: the spin-echo, where the coherence order changes by $\Delta p = +1$, the FID from the second pulse, where $\Delta p = 0$, and the FID from the first pulse, where $\Delta p = +1$. For each pathway, we define the quantity $P(\{\Delta\varphi_i\}, \{\theta_i\}, \Delta p)$ given by

$$P(\{\Delta\varphi_i\}, \{\theta_i\}, \Delta p) = \frac{1}{4}\sum_{i=0}^{3} \exp(-i(\Delta p \Delta\varphi_i + \theta_i)) \tag{7}$$

where $\{\Delta\varphi_i\}$ is the set of four phases through which the first pulse is cycled, and $\{\theta_i\}$ is the set of four receiver phases applied to the complex data in post-processing. The complex coefficients $P(\{\Delta\varphi_i\}, \{\theta_i\}, \Delta p)$ are the weights of the contribution from each coherence transfer pathway Δp. The goal of POPS is to have

$$P(\{\Delta\varphi_i\}, \{\theta_i\}, \Delta p) = \begin{cases} 1 & \text{Desired } \Delta p \\ 0 & \text{Undesired } \Delta p \end{cases} \tag{8}$$

The task is therefore to find the optimal set of receiver phases $\{\theta_i\}$ to satisfy Equation 8.

Least-squares method

The least-squares method of assigning receiver phases seeks to satisfy 7 in a least-squares sense. If the desired coherence transfer pathway is labeled with Δp and the undesired pathways with $\Delta p'$, then the least-squares method seeks a set of phases $\{\theta_i\}$ which minimize the real and imaginary parts of the coefficients $P(\{\Delta\varphi_i\}, \{\theta_i\}, \Delta p')$ corresponding to the unwanted coherences, while minimizing the real and imaginary parts of $P(\{\Delta\varphi_i\}, \{\theta_i\}, \Delta p) - 1$, corresponding to the wanted coherence. This procedure seeks both to remove contributions from undesired coherences, and to correctly set the phase of the resulting signal. The least-squares method was carried out using a Levenberg-Marquardt algorithm, implemented in python using the curve_fit function from the scipy library.

The algorithm was provided with a suitable guess for the receiver phases in the form of the phases satisfying the following equations

$$\Delta\varphi_0 = \Delta\varphi_2 + \pi \mod 2\pi \tag{9a}$$

$$\Delta\varphi_1 = \Delta\varphi_3 + \pi \mod 2\pi \tag{9b}$$

$$\theta_0 + \Delta p \Delta\varphi_0 = \theta_1 + \Delta p(\Delta\varphi_1 + \pi) \mod 2\pi \tag{9c}$$

$$\theta_2 + \Delta p \Delta\varphi_2 = \theta_3 + \Delta p(\Delta\varphi_3 + \pi) \mod 2\pi \tag{9d}$$

in a least squares sense,

$$\vec{\theta} = (A^T A)^{-1} A^T \vec{X}_{\Delta p} \tag{10}$$

where

$$A = \begin{pmatrix} 1 & 0 & -1 & 0 \\ 0 & 1 & 0 & -1 \\ 1 & -1 & 0 & 0 \\ 0 & 0 & 1 & -1 \end{pmatrix} \tag{11a}$$

$$\vec{X}_{\Delta p} = \begin{pmatrix} \Delta p \pi \\ \Delta p \pi \\ \Delta p(\Delta\varphi_0 - \Delta\varphi_1 - \pi) \\ \Delta p(\Delta\varphi_2 - \Delta\varphi_3 - \pi) \end{pmatrix} \tag{11b}$$

where $\vec{\theta} = (\theta_0, \theta_1, \theta_2, \theta_3)$.

Echo-optimized method

The echo-optimized method seeks to completely remove contributions to the final signal from the unwanted FIDs generated by each pulse. This is accomplished by both phase-shifting and amplitude-scaling, in contrast to the least-squares method, which only uses phase-shifting.

POPS APPLIED TO DIAMOND P1 CENTERS

Figure S2 shows how phase cycling was carried out for the two-pulse experiments performed on P1 centers in diamond. Figure S2a shows the time-traces acquired for each

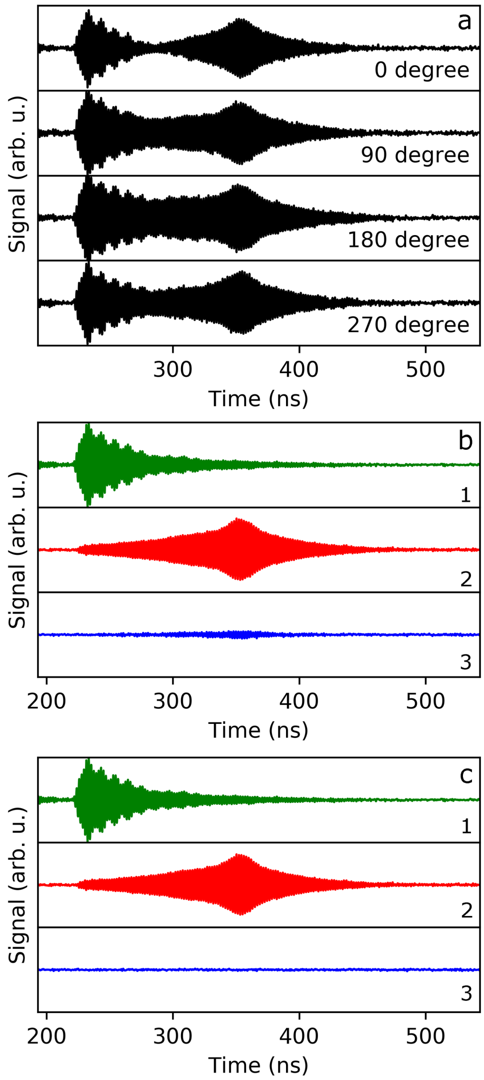

FIG. S2: (a) Four signals, generated using phase shifter plates designed produce phase shifts of $0°, 90°, 180°$, and $270°$, as labeled. The actual phase shifts $\Delta\varphi$ were measured to be $0°, 79°, 179°$, and $252°$. Each trace is the average of experiments scans. (b) Summed signals from (a) after numerical phase shifts $\{\theta_i\}$ have been applied in post processing to each trace, where $\{\theta_i\}$ were chosen assuming the pulse phase shifts were $0°, 90°, 180°$, and $270°$. (c) Summed signals from (a) after numerical phase shifts $\{\theta_i\}$ have been applied in post processing to each trace, where $\{\theta_i\}$ were chosen based on the measured pulse phases using the least-squares method.

applied phase shift $\Delta\varphi_i$, where phase shifter plates were used to generate shifts in the phase of the first pulse of $0°, 79°, 179°$, and $252°$. Figure S2b shoes the three summed signals generated from the time-domain traces shown in S2a after applying numerical phase shifts $\{\theta_i\}$ to select (1) the FID from the second pulse, (2) the echo, and (3) the FID from the first pulse, where $\{\theta_i\}$ were chosen assuming the pulse phase shifts were $0°, 90°, 180°$, and $270°$. To select the FID from the second pulse, the numerical phase shifts $\{\theta_i\}$ which were applied were $\{0°, 0°, 0°, 0°\}$. To select the echo, the numerical phase shifts $\{\theta_i\} = \{0°, 270°, 180°, 90°\}$ were applied. To select the FID from the first pulse, the numerical phase shifts $\{\theta_i\} = \{0°, 900°, 180°, 270°\}$ were applied. The FID from the first pulse has decayed below the detection threshold, however there is still some apparent signal in Figure S2b-3, at the location of the echo.

Figure S2c shows the three summed signals generated from the time-domain traces shown in S2a after applying numerical phase shifts $\{\theta_i\}$ calculated using the least-squares method. To select the FID from the second pulse as shown in Figure S2c-1, the numerical phase shifts $\{\theta_i\} = \{354.0°, 6.8°, 352.4°, 6.8°\}$ were applied. To select the echo as shown in Figure S2c-2, the numerical phase shifts $\{\theta_i\} = \{13.5°, 270.8°, 193.6°, 91.2°\}$ were applied. To select the FID from the first pulse as shown in S2c-3, the numerical phase shifts $\{\theta_i\} = \{346.5°, 89.2°, 166.4°, 268.8°\}$ were applied.

REFERENCES

[1] J. Birch, J. Dromey and J. Lesurf, *Infrared Physics*, 1981, **21**, 225 – 228.

[2] R. Piesiewicz, C. Jansen, S. Wietzke, D. Mittleman, M. Koch and T. Kürner, *International Journal of Infrared and Millimeter Waves*, 2007, **28**, 363–371.

[3] D. T. Edwards, Y. Zhang, S. J. Glaser, S. Han and M. S. Sherwin, *Phys. Chem. Chem. Phys.*, 2013, **15**, 5707–5719.